

Micro-well arrays for 3D shape control and high resolution analysis of single cells†

Mirjam Ochsner,^a Marc R. Dusseiller,^a H. Michelle Grandin,^a Sheila Luna-Morris,^b Marcus Textor,^a Viola Vogel^b and Michael L. Smith^{*b}

Received 26th March 2007, Accepted 6th June 2007

First published as an Advance Article on the web 21st June 2007

DOI: 10.1039/b704449f

In addition to rigidity, matrix composition, and cell shape, dimensionality is now considered an important property of the cell microenvironment which directs cell behavior. However, available tools for cell culture in two-dimensional (2D) *versus* three-dimensional (3D) environments are difficult to compare, and no tools exist which provide 3D shape control of single cells. We developed polydimethylsiloxane (PDMS) substrates for the culture of single cells in 3D arrays which are compatible with high-resolution microscopy. Cell adhesion was limited to within microwells by passivation of the flat upper surface through ‘wet-printing’ of a non-fouling polymer and backfilling of the wells with specific adhesive proteins or lipid bilayers. Endothelial cells constrained within microwells were viable, and intracellular features could be imaged with high resolution objectives. Finally, phalloidin staining of actin stress fibers showed that the cytoskeleton of cells in microwells was 3D and not limited to the cell–substrate interface. Thus, microwells can be used to produce microenvironments for large numbers of single cells with 3D shape control and can be added to a repertoire of tools which are ever more sought after for both fundamental biological studies as well as high throughput cell screening assays.

Introduction

Early efforts to determine how cell adhesion and shape impact cell function were complicated by rudimentary tools which, for instance, were incapable of differentiating between the effects of ligand density from the extent of cell spreading.¹ A new generation of tools can be used to produce spatially confined islands of adhesive ligands surrounded by a non-fouling background on surfaces with variable elasticity.² Such tools were used to show that by constraining cell shape or the degree of spreading one can steer cells to either proliferate or to undergo apoptosis³ and can even direct differentiation of human mesenchymal stem cells.⁴ However, studies on the relationship between shape and cell behavior have thus far been limited to 2D surfaces.

A new consensus expresses that there are fundamental differences between cells grown in 2D *versus* 3D.^{5,6} Cells cultured on cell-derived 3D matrices show differences in the phenotype of cell–matrix adhesions,⁶ and differences in gene expression have been observed for cells cultured in 2D *versus* 3D.⁷ Although synthetic hydrogels and fibrous collagen-based matrices provide physiologically relevant 3D environments for cells, these systems cannot be used to control cell shape and

may have altered local mechanical properties as cells remodel their surroundings.

Microwells provide a novel approach for 3D cell culture^{8,9} which can be more directly compared with 2D surfaces since in both cases cells are in contact with planar surfaces coated with adhesive ligands. Innovative approaches to trap single cells in microwells have been developed and optimized for a high rate of well occupancy by single cells.^{10–13} However, these approaches are better suited for the generation of population statistics derived from individual cell measurements than for basic biological investigations since they have yet to be adapted for 3D shape control¹⁴ and few of these approaches are compatible with high resolution microscopy.¹³ The main objective of our work was to develop a platform with variable substrate elasticity and high resolution microscopic compatibility which can be used to control the 3D shape of cells.

Materials and methods

Microwell fabrication

Arrays of microwells with different geometries (circles, squares, triangles, rectangles, spindles, *etc.*), lateral dimensions (81 μm^2 to 900 μm^2 area on mask) and a depth of 10 μm were first produced in Silicon using standard photolithography and inductively coupled plasma etching (ICP),¹⁵ and polydimethylsiloxane (PDMS) replicas were cast (1 : 10, curing agent to prepolymer). After fluorosilanization of this first PDMS master (1H,1H,2H,2H- Perfluorooctyltrichlorosilane, ABCR GmbH, Germany), thin films of PDMS were replicated on a glass coverslip (Menzel-Gläser, Germany, strength 0, approx. 100 μm thickness) which was fixed on a glass support for

^aBioInterface Group, Laboratory for Surface Science and Technology, ETH Zurich, CH-8093, Zürich, Switzerland

^bLaboratory for Biologically Oriented Materials, Department of Materials, Swiss Federal Institute of Technology, ETH Zurich, Hönggerberg, CH-8093, Zürich, Switzerland.

E-mail: michael.smith@mat.ethz.ch; Tel: +41 (0)44 633 6927

† Electronic supplementary information (ESI) available: Details of fibronectin isolation and fluorescent labeling, scanning electron microscopy, PDMS stiffness and Figs. S1–S4. See DOI: 10.1039/b704449f

stability. A drop of PDMS was cast on the coverslip while 70 μm coverslips (Menzel-Gläser, Germany, strength 00) were used as spacers (Fig. 1A). The master was weighted with 120 g (Fig. 1B). After curing the PDMS, the 1st PDMS master was peeled off and the PDMS film remained stuck to the underlying coverslip. The sandwich was removed from the support (Fig. 1C) and glued with PDMS to the bottom of a petri dish into which an aperture was previously drilled (Fig. 1D), and a PDMS ring was added for fluid containment. Finally, the culture dishes were sterilized with 70% ethanol/water before surface functionalization and cell culture.

Surface functionalization

To passivate the plateau of the PDMS chips and to render it resistant to protein adsorption and cell adhesion, a polyacrylamide (PAAm) hydrogel based inverted microcontact printing method was developed. To obtain a protein resistant surface, 50 μl of 20 $\mu\text{g ml}^{-1}$ poly(L-lysine)-graft-poly(ethylene glycol) (PLL-g-PEG; (20)-[3.3]-(2); SurfaceSolutions, Switzerland) in phosphate buffered saline (PBS; Fluka, Switzerland) was added to 1 ml of PAAm pre-gel (30% Acrylamide 4 K-Solution Mix 37.5 : 1; AppliChem, Germany) and the crosslinking reaction was started by addition of 10 μl of ammonium persulfate (Aldrich, Germany) and 2 μl of *N,N,N,N*-tetramethyl ethylenediamine (Sigma, Germany). The PLL-g-PEG-PAAm hydrogel was then cast and cured. The microstructured PDMS surface was exposed to air plasma at 0.1 mbar for 30 s (PDC-32G Harrick Scientific) to create negative charges at the surface for the electrostatically driven adsorption of the positively charged PLL-g-PEG backbone.¹⁶ The substrate was stamped upside down for 15 min with a 5 g weight (Fig. 1E).

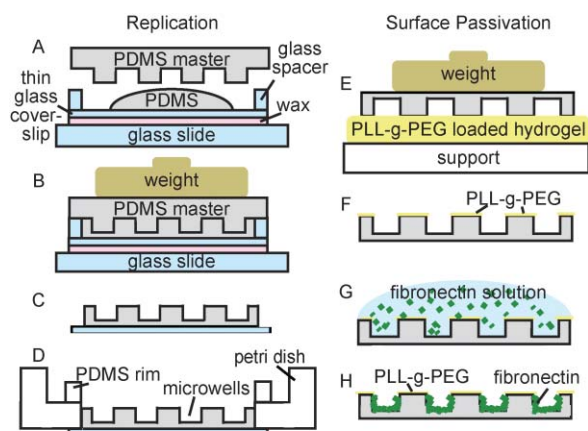


Fig. 1 In order to produce microwells in thin films of PDMS, a thin glass coverslip is glued onto a glass specimen slide between which the PDMS is cast (A). This sandwich is weighted while the PDMS is cured (B). The master and glass support are removed leaving behind a thin PDMS film bound to the coverslip (C) which is then glued to the bottom of a Petri dish into which a hole was drilled (D). The microwell plateau surface is passivated by inverted micro-contact printing of PLL-g-PEG using a PAAm stamp (E). After plateau passivation (F) the sample is exposed to a Fn solution (G), and after rinsing only the microwell surfaces are coated with Fn (H).

After passivation of the background (Fig. 1F), the sample was exposed to 25 $\mu\text{g ml}^{-1}$ unlabeled or fluorescently labeled fibronectin (Fn) (see ESI†) in PBS for 1 h (Fig. 1G) or to 0.1 g l^{-1} of extruded (Lipofast extruder, Avestin, Canada) 50 nm diameter 1,2-dioleoyl-sn-glycero-3-phosphocholine (DOPC; Avanti Polar Lipids, USA) vesicles for 10 min. Fn and lipid bilayers were limited to the non-passivated microwell walls by PLL-g-PEG passivation of the top surface (Fig. 1H). DOPC bilayers were characterized by quartz crystal microbalance with dissipation and fluorescence recovery after photobleaching.

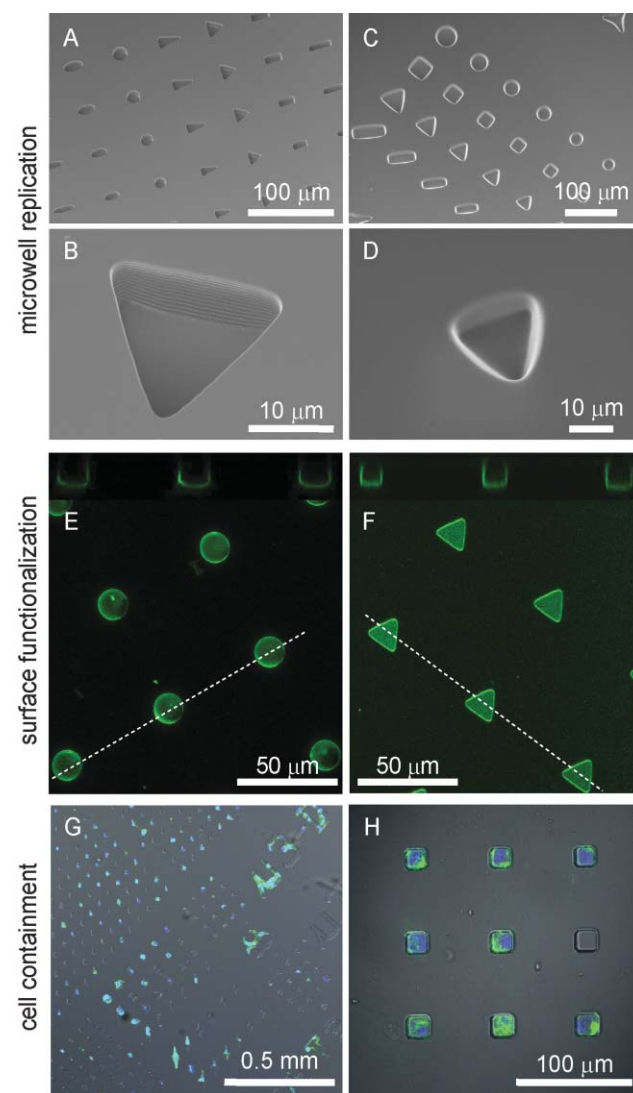


Fig. 2 Scanning electron microscopy images are shown of PDMS replicas of the microfabricated wells of various shapes in hard (A, B; ~ 1.3 MPa) and soft PDMS (C, D; ~ 10 kPa). Maximum intensity projections and cross-sections of confocal laser scanning microscopic z-stack images of microwells coated with labeled Fn (E) and labeled DOPC bilayers (F) are shown. Overlays of DIC and fluorescent confocal images acquired with 10 \times air (G) and 60 \times oil (H) objectives are shown of HUVECs in microwells stained with Alexa 488-phalloidin (actin; green) and ethidium homodimer (nuclei; blue) after 24 h of culture.

Results and discussion

In order to generate arrays of microwells which could be used to constrain cell shape in 3D, a silicon master was produced using standard photolithography and ICP followed by replication into a 1st PDMS master and finally into the PDMS sample. A thin film replication technique was developed to permit high resolution microscopy of samples (Fig. 1A–D). The fidelity of the microstructures as assessed by scanning electron microscopy was very high (see ESI† and Fig. 2A–D). Replication of hard PDMS (1 : 10 mixture) led to microwells with straight walls containing sub-micrometer scallops resulting from ICP etching of a Si master (Fig. 2B). Soft structures (1 : 40 and 1 : 60) showed less accurate retention of shape fidelity due to the low stiffness of the resulting polymer (Fig. 2C, D). Substrate stiffness could be varied from ~ 1.3 MPa (1 : 10) to 4 kPa (1 : 60; see ESI Fig. S1), although Young's moduli were lower than previously published measurements. For example, 1 : 50 ratios yielded ~ 8 kPa, while other studies reported values from 12–48 kPa.^{17–19}

Wet-printing of PLL-g-PEG by inverted microcontact printing was developed for the passivation of the upper plateau surface (Fig. 1E–H). Fig. 2E demonstrates that microwells could be specifically backfilled with fluorescent Fn, while the PLL-g-PEG coated plateau surface was Fn resistant. As many proteins of interest in cell studies are transmembrane proteins where ligand mobility may be important, microwells were also coated with lipid bilayers (Fig. 2F). Prevention of cell adhesion by PLL-g-PEG was investigated by incubating primary human umbilical vein endothelial cells (HUVEC; see ESI†) for 30 min followed by gentle rinsing to remove nonadherent cells. Cell attachment

and spreading were predominantly limited to within Fn coated microwells even after 24 h in culture (Fig. 2G, H).

Cell confinement in 3D is only completely controlled by microwells when cell and microwell volumes are similar (see ESI Fig. S2†). Rettig *et al.* demonstrated that the total percentage of microwells filled by single cells could be optimized by modulating cell seeding conditions and microwell dimensions.¹² The approach presented here utilized smaller microwells than previous studies in order to match cell and microwell volumes. Thus, an array of different dimensions was fabricated so that different cell lines with variable cell volumes could be used on the same platform. In addition, the upper surface passivation approach developed here can be used with variable spacing between microwells, for instance to investigate paracrine signaling effects between cells in wells. With the seeding and incubation times used here, $\sim 45\%$ of microwells were occupied by HUVECs (Fig. 2G, H), however future platform designs could utilize a narrower range of microwell sizes tuned for a specific cell type in order to optimize single cell occupancy for high throughput applications.¹²

To test whether the microwell approach is compatible with high resolution microscopy, intracellular features were imaged by phalloidin and ethidium homodimer staining of actin and nuclei, respectively, with a $60\times$ oil objective (see ESI†). Control experiments demonstrated that diffusive limitations of the microwell platform did not limit the ability to visualize Fn bound under cells in wells (see ESI Fig. S3†). In addition, HUVECs were viable in microwells (see ESI Fig. S4†) after 24 h culture. In contrast to very large microwells where cells formed a monolayer as in traditional 2D cultures (Fig. 3A), the actin cytoskeleton of cells whose 3D shapes were fully confined by microwells were remarkably 3D, and prominent actin stress

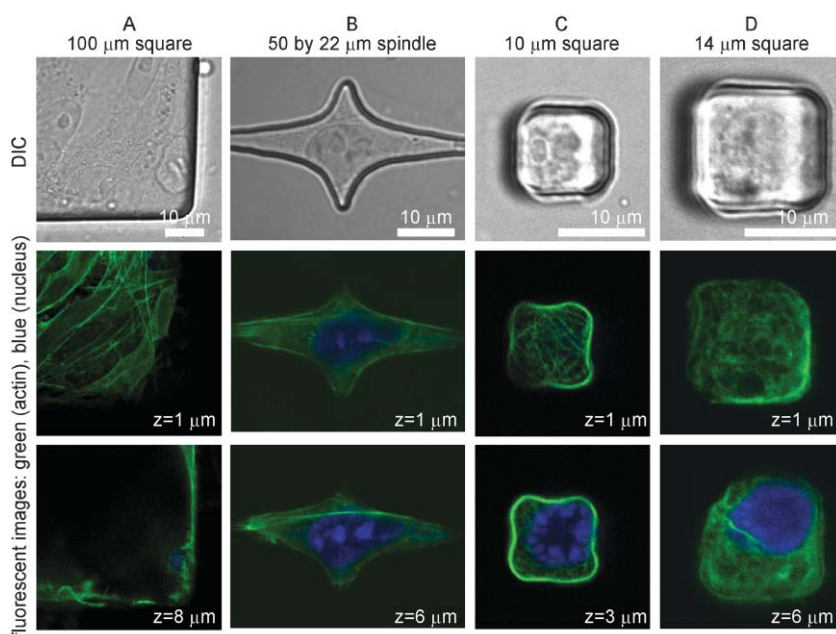


Fig. 3 DIC and fluorescent confocal images are shown of cell nuclei (ethidium homodimer; blue) and actin cytoskeletal networks (Alexa 488-phalloidin; green). HUVECs cultured for 24 h are shown in a large microwell (A), a spindle-shaped microwell which was slightly bigger than the confined cell (B), and 10 (C) and 14 μm square (D) microwells which adequately controlled the 3D shape of cells. Confocal slices are shown at different height positions in the microwells where $z = 0$ indicates the microwell bottom.

fibers were often aligned along the long axis of the microwell (Fig. 3B–D). In addition, nuclear shape could easily be resolved inside microwells and was often similar to that of the microwell (Fig. 3C).

Conclusion

Two-dimensional surfaces with variable elasticity or patterned ECM ligands opened a new dimension in our understanding of the relationship between the physical form of the local cell microenvironment and cell fate. However, cell behavior in 3D cannot be predicted with 2D systems, and new tools which allow independent modulation of cell shape and rigidity in 3D are needed. The microwell platform developed here allows for 3D shape control of single cells with variable substrate elasticity and can now be used to address a host of biological questions from the mechanism of dimensionality sensation to the impact of 3D cell shape on cell orientation during division.

Acknowledgements

We gratefully acknowledge Jérôme Lefèvre for assistance with elasticity measurements. This study was supported by the ETH Zurich, the Swiss National Science Foundation (FN 205321-112323/1; MO), the Swiss Competence Centre for Materials Science and Technology (CCMX) and the International Human Frontier Science Program Organization (MLS).

References

- 1 J. Folkman and A. Moscona, *Nature*, 1978, **273**, 345–349.
- 2 D. Falconnet, G. Csucs, H. M. Grandin and M. Textor, *Biomaterials*, 2006, **27**, 3044–3063.
- 3 C. S. Chen, M. Mrksich, S. Huang, G. M. Whitesides and D. E. Ingber, *Science*, 1997, **276**, 1425–1428.
- 4 R. McBeath, D. M. Pirone, C. M. Nelson, K. Bhadriraju and C. S. Chen, *Dev. Cell*, 2004, **6**, 483–495.
- 5 L. G. Griffith and M. A. Swartz, *Nat. Rev. Mol. Cell Biol.*, 2006, **7**, 211–224.
- 6 E. Cukierman, R. Pankov, D. R. Stevens and K. M. Yamada, *Science*, 2001, **294**, 1708–1712.
- 7 A. Birgersdotter, R. Sandberg and I. Ernberg, *Semin. Cancer Biology*, 2005, **15**, 405–412.
- 8 C. E. Sims and N. L. Allbritton, *Lab Chip*, 2007, **7**, 423–440.
- 9 D. Di Carlo and L. P. Lee, *Anal. Chem.*, 2006, **78**, 7918–7925.
- 10 A. Revzin, K. Sekine, A. Sin, R. G. Tompkins and M. Toner, *Lab Chip*, 2005, **5**, 30–37.
- 11 E. Ostuni, C. S. Chen, D. E. Ingber and G. M. Whitesides, *Langmuir*, 2001, **17**, 2828–2834.
- 12 J. R. Rettig and A. Folch, *Anal. Chem.*, 2005, **77**, 5628–5634.
- 13 V. I. Chin, P. Taupin, S. Sanga, J. Scheel, F. H. Gage and S. N. Bhatia, *Biotechnol. Bioeng.*, 2004, **88**, 399–415.
- 14 M. Dusseiller, M. L. Smith, V. Vogel and M. Textor, *Biointerphases*, 2006, **1**, P1–P4.
- 15 M. R. Dusseiller, D. Schlaepfer, M. Koch, R. Kroschewski and M. Textor, *Biomaterials*, 2005, **26**, 5917–5925.
- 16 S. Pasche, S. M. De Paul, J. Voros, N. D. Spencer and M. Textor, *Langmuir*, 2003, **19**, 9216–9225.
- 17 N. Q. Balaban, U. S. Schwarz, D. Riveline, P. Goichberg, G. Tzur, I. Sabanay, D. Mahalu, S. Safran, A. Bershadsky, L. Addadi and B. Geiger, *Nat. Cell Biol.*, 2001, **3**, 466–472.
- 18 D. S. Gray, J. Tien and C. S. Chen, *J. Biomed. Mater. Res., A*, 2003, **66**, 605–614.
- 19 X. Q. Brown, K. Ookawa and J. Y. Wong, *Biomaterials*, 2005, **26**, 3123–3129.